

SCANDINAVIAN BAFFLE BOILER DESIGN REVISITED

by

Borivoj Lj. STEPANOV*, **Ivan K. PEŠENJANSKI**,
and Momčilo Dj. SPASOJEVIĆ

Faculty of Technical Sciences, Novi Sad, Serbia

Original scientific paper
DOI: 10.2298/TSC1130508070S

The aim of this paper is to examine whether the use of baffles in a combustion chamber, one of the well-known low-cost methods for the boiler performance improvement, can be enhanced. Modern day tools like computational fluid dynamics were not present at the time when these measures were invented, developed, and successfully applied. The objective of this study is to determine the influence of location and length of a baffle in a furnace, for different mass flows, on gas residence time. The numerical simulations have been performed of a simple Scandinavian stove like furnace. The isothermal model is used, while air is used as a medium and turbulence is modeled by realizable k - ϵ model. The Lagrange particle tracking is used for the residence time distribution determination. The statistical analysis yielded the average residence time. The results of the computational fluid dynamics studies show that influence of baffle positions, dimension, and flow rates can decrease residence time even 17% but also increase it up to 13%. Vertical position of the baffle is the most important factor, followed by the length of the baffle, while the least important showed to be the mass flow.

Key words: *combustion improvement, residence time, baffle, cold flow, computational fluid dynamics*

Introduction

Biomass as a fuel, when compared to coal, has a lower energy density thus being more difficult to handle. Its chemical composition causes deposits resulting from combustion which in turn lead to slagging and fouling as the problems with which engineers are confronted. The important property of a straw is its volatile content. For the wheat straw, volatile content is 71%, ash 8.9%, fixed carbon 20%, according to [1]. Similar data can be found in [2]. In other words, we are dealing with approximately gaseous-like solid fuel, and this fact should be taken into account when designing a furnace, if efficient and eco-friendly boiler is to be made.

According to the performed tests reported in [3, 4], the efficiencies of straw bales boilers in Serbia are in the range from 31 to 73%, while the excess air values, on the other hand, are in the range from 1.3 to 8.8%. These boilers are provided with a simple fire-box design and water cooled walls but they lack baffles. They are operated with high air excess values to achieve targeted heat outputs which as a consequence have low efficiency. These results show that there is a great margin for an improvement. As these boilers are in the low-cost segment, logical choice are low-cost solutions. Baffles represent one potential opportunity.

* Corresponding author; e-mail: bstep@uns.ac.rs

The usage of baffles was introduced by the Norwegian company Jotul in stoves design in the 1970s in the time of oil crisis. A baffle forces gases to take the longer path before exiting the combustion chamber. This is presented in fig. 1B. Similar design but with vertical baffle is presented in fig. 1D. Both mentioned designs have their simple forms presented in figs. 1A and 1C. It causes an increase in the pressure drop, however the effect on the extent of dead and re-circulation zones is still unknown. Combustion efficiency can be improved, either by better mixing of the reactants, increase of turbulence intensity or by gas temperature increase in the primary zone. Temperature barrier between primary zone and cooled parts of the furnace has to be introduced.

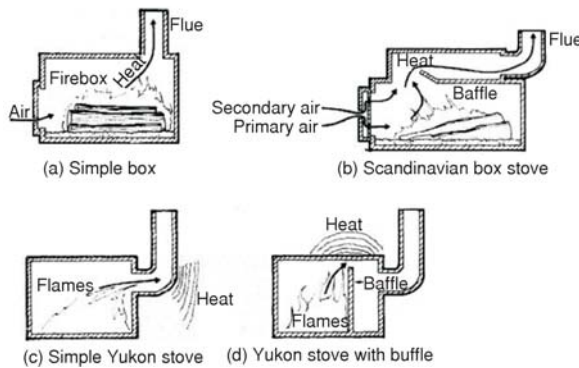


Figure 1. Stove designs with and without baffles [5]

There is a common misconception that baffles increase the residence time per se, but the value that is actually increased is the gas flow path. In order to calculate the residence time, information about the velocity field is necessary [6-8].

Temperature, turbulence, and residence time are the crucial factors which have to be taken into account when designing an efficient boiler furnace. An increase of the residence time leads to better combustion, a step closer to the complete one and also provides the possibility of using lower air excess values,

which from the abovementioned measurements can in practice turn boiler into an air heater.

The resident time of effluent streams from real combustors varies, and one way to deal with this problem is by using distribution functions, *i. e.* by the introduction of statistical methods.

The residence or retention time in a combustion chamber without baffles can be estimated through the division of chamber volume with the volumetric flow rate. The question remains what is the extent of dead zones in which re-circulating eddies form. These are causing the lower effective volume and influence the residence time.

In the incinerator industry the residence time has been increased by the method of cyclonic flow induction which is achieved by appropriate locations and orientations of burners.

The ratio between the furnace volume that is occupied by flue gases and the furnace volume is in the range 0.8 to 1 for solid fuel combustion [9]. Therefore, one of the design goals is to increase this ratio as, in that case, time left for combustion is greater. This data is for larger boiler units, the ones that are used in industry and utilities.

The publications on performed tests on baffles are rare.

Data is available from the producer Jotul. An experiment was organized in Canada, where two cast-iron stoves were installed in identical buildings 1.5 km apart. These stoves are schematically shown in fig. 1A and B. One unit was without baffles and provision of secondary air and the other was Jotul No. 118 that has horizontal baffle and a hollow door that serves a purpose of preheating air. Air in this stove is split in two streams through two ports on the inside of the door. The upper port is for secondary air, and the lower port is for primary air. Results showed that Jotul No. 118 consumed 0.12 cubic meters of wood per day, and conventional stove used 0.24 cubic meter.

Additional test results can be found in [8], where results of a study in which large number of test is performed on different stoves. The conclusions drawn from the tests point out the unpredictability of the baffle effect, as there are so many design configurations possible. The results from one of the tests of two Scandinavian stoves are presented. These two stoves, which differentiate in size, are of the same design. The tests were performed with and without baffle presence, as well as over a range of power inputs. The results show the following effects. In a larger stove, baffle had little effect on any of the three energy efficiencies – combustion, heat transfer, and overall. In the case of the smaller stove, overall energy efficiency is improved by 2 percentage points.

Figure 2 shows how many design variations baffle can create to a simple combustion/heating device – vertical drum stove. This type is not further analyzed and simulated in this paper.

Baffles are present in the contemporary design, which can be seen in a number of studies where this design detail is present [10-12], as well as in the modern biomass boilers. In studies [13, 14] problem of maximizing residence time of combustion gases in the secondary chamber by improving fire-box configuration and baffle locations is stated. In the [15] the flow in stoves with baffles is known under name S-flow. The residence time was studied in the 60 and 70-s [16, 17]. It is worth mentioning that the cold flow approach was implemented in [16].

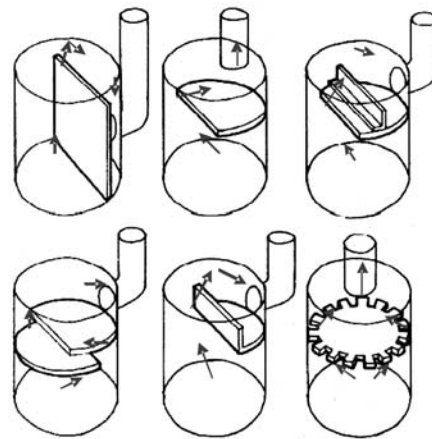


Figure 2. Various baffle arrangements for vertical drum stoves [5] Arrows represent flue gas flow

Method

Model description

In this study commercial STAR-CCM+ software is used. Its CFD solver is used for solving problems involving flow (of fluids or solids), heat transfer and stress. It has ability to tackle problems involving multi-physics and complex geometries.

Flow in combustion chamber is described by system of differential equations, Reynolds averaged Navier-Stokes equations:

$$\frac{\partial}{\partial x_i} (\rho u_i) = 0 \quad (1)$$

$$\frac{\partial}{\partial x_j} (\rho u_i u_j) = -\frac{\partial P}{\partial x_i} + \frac{\partial}{\partial x_j} \left[\mu \left(\frac{\partial u_i}{\partial x_j} + \frac{\partial u_j}{\partial x_i} - \frac{2}{3} \delta_{ij} \frac{\partial u_i}{\partial x_j} \right) \right] + \frac{\partial}{\partial x_j} (-\rho \overline{u_i' u_j'}) \quad (2)$$

As a result of Reynolds averaging additional terms appear – Reynolds' stresses.

$$\mathbf{T}_t \equiv -\rho \overline{u_i' u_j'} \quad (3)$$

Reynolds stress tensor:

$$\mathbf{T}_t = \mu_t \left(\frac{\partial u_i}{\partial x_j} + \frac{\partial u_j}{\partial x_i} \right) - \frac{2}{3} \left(\rho k + \mu_t \frac{\partial u_i}{\partial x_j} \right) \delta_{ij} \quad (4)$$

where k is the turbulent kinetic energy.

Eddy viscosity models use the concept of a turbulent viscosity to model the Reynolds stress tensor as a function of mean flow quantities.

Turbulent viscosity is defined as:

$$\mu_t = \rho C_\mu \frac{k^2}{\varepsilon} \quad (5)$$

Closure of the RANS equation is obtained through solution of additional transport equations for scalar quantities that enable the turbulent viscosity to be derived.

Used realizable k - ε turbulence model is a two-equation model in which transport equations are solved for the turbulent kinetic energy k (eq. 6) and its dissipation rate ε (eq. 7). Difference between the standard and realizable k - ε models is in inclusion of C_μ dependence of mean flow and turbulence properties.

The realizable two-layer k - ε model combines the realizable k - ε model with the two-layer approach:

$$\frac{\partial}{\partial t}(\rho k) + \frac{\partial}{\partial x_j}(\rho k u_j) = \frac{\partial}{\partial x_j} \left[\left(\mu + \frac{\mu_t}{\sigma_k} \right) \frac{\partial k}{\partial x_j} \right] + G_k + G_b - \rho \varepsilon - Y_M + S_k \quad (6)$$

$$\frac{\partial}{\partial t}(\rho \varepsilon) + \frac{\partial}{\partial x_j}(\rho \varepsilon u_j) = \frac{\partial}{\partial x_j} \left[\left(\mu + \frac{\mu_t}{\sigma_\varepsilon} \right) \frac{\partial \varepsilon}{\partial x_j} \right] + \rho C_1 S_\varepsilon - \rho C_2 \frac{\varepsilon^2}{k + \sqrt{\nu \varepsilon}} + C_{1\varepsilon} \frac{\varepsilon}{k} C_{3\varepsilon} P_b + S_\varepsilon \quad (7)$$

where

$$C_1 = \max \left[0.43 \frac{\eta}{\eta + 5} \right], \quad \eta = S \frac{k}{\varepsilon}, \quad S = \sqrt{2 S_{ij} S_{ij}} \quad (8)$$

$$C_{1\varepsilon} = 1.44, \quad C_2 = 1.9, \quad \sigma_k = 1.0, \quad \sigma_\varepsilon = 1.2 \quad (9)$$

Cold flow approach

Cold flow is known by other names: isothermal flow, non-reacting flow, and they all refer to modeling flow without taking into account the reactions.

In order to determine the effects of design parameters on combustion, researchers have frequently used cold-flow simulations. The examples are referenced in [18], and these are works from the field of waste incineration [19-23]. The cold flow models are extremely useful, because they provide a reasonable amount of information while minimizing the complexities and efforts [18].

It is obvious, however, that the real incinerator performance cannot be reproduced with cold-flow models. Some of the major problems include: the density variation of combustion gases (typically a function of the temperature and the combustion stoichiometry), the heat generation associated with the chemical reaction and the heat transfer between the wall, the waste bed and the combustion gases (probably with the products of incomplete combustion) [18]. Independently from the above stated, the recommendation has been made [24] to include dependence of gases density on height in the model. However, convergence difficulties have been present.

It is of importance to note the example from industry, in which Steinmueller, a renowned incinerator producer, relied heavily on extensive cold-flow modeling and in-furnace measurements to optimize the design and operation of their systems in order to ensure high temperatures and uniform mixing conditions [25].

Residence time calculation

STAR-CCM+ uses Lagrangian/Eulerian framework [26] for describing multiphase problems. The physics continuum is a continuous phase whose governing equations are expressed in Eulerian form. The Lagrangian approach is applied for modeling of arbitrary number of dispersed phases. Particle-like elements known as parcels are followed through the continuum, with the state of each parcel updated according to a selected set of models and optionally recorded as a track.

These discrete phases can be with or without mass. In this paper massless phase has been utilized. These massless particles are moving with the continuous phase. They do not influence each other or the continuous phase. The velocity of the massless particle is equal to the one of the surrounding fluid:

$$u_p = u \quad (10)$$

Data about the particle flow is recorded in a file named particle track. Particle track can contain residence time and coordinates data. This data can be exported in commas separated format, where data for each particle track is given sequentially. For one particle track, for each substep, the residence time spent during this substep is calculated, by knowing the length of a substep path and velocity. This value is added to the previous value, thus the result is the particle residence time from the inclusion point to the current position. The coordinates are also recorded, thus they can be used to correlate residence time data with the length of particle tracks.

This data is analyzed in MS Excel. After the last residence time value for every particle track is extracted they are sorted for the purpose of the data analysis. Finally, the calculation of the average residence time is performed. The number of the total number of sub-steps changes from one to another particle track. Most of the particle tracks reach exit from the chamber, and some enter the stagnation or re-circulation zone.

Two parameters are of great importance for the residence time calculation: maximum number of substeps, and maximum residence time. When either of them is reached, the Lagrangian solver stops, and the last value calculated and recorded is treated as the residence time. In these simulations maximum number of substeps was 10000, and the maximum residence time was set to 100 s.

Description of geometry, mesh, and boundary conditions

Nine different geometry cases have been studied, each determined by the vertical position and the length of the baffle. In each case baffle extends from back side of the furnace. The dimensions are: $1 \times 1 \times 1$ m (height \times width \times length). Model is three-dimensional. Figure 3 represents Scandinavian stove and fig. 4. represents a simplified boiler furnace that utilizes baffle design. There is a difference in the place where the exit section is located. In fig. 3 it is positioned on the back side, and in the model it is on the top side. Additional difference is the point of entry of air. Air in the boiler furnace enters through the grate which is

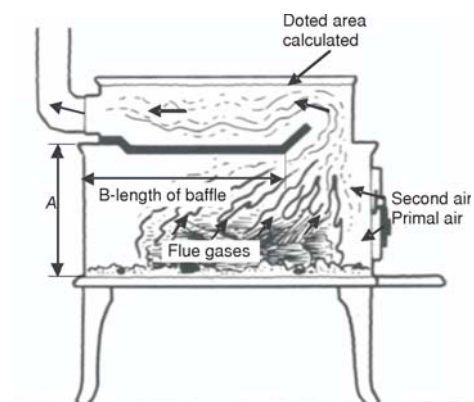


Figure 3. Scandinavian stove [7]

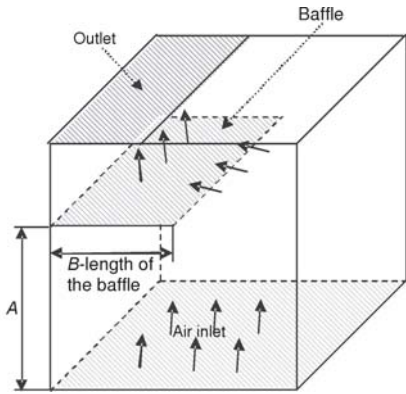


Figure 4. Geometry of the problem

represented by the bottom plane. The recommended furnace heat load per volume unit is taken from [27] for the hand stoked boilers. For the given heat load according air flows are calculated for different air excess values. They are 0.16, 0.24, 0.32, 0.40, and 0.48 kg/s.

The two main parameters determine the geometry. It is A which is the height at which the baffle is positioned in the firebox, and B which is the width of the baffle. The A parameter in the simulations takes the values: A1 – 0.7 m, A2 – 0.8 m, A3 – 0.9 m, and the B parameter takes: B1 – 0.7 m, B2 – 0.8 m, B3 – 0.9 m. The combination of these values leads to the cases: Case 1 – A1 & B1, Case 2 – A1 & B2, Case 3 – A1 & B3, Case 4 – A2 & B1, Case 5 – A2 & B2, Case 6 – A2 & B3, Case 7 – A3 & B1, Case 8 – A3 & B2, Case 9 – A3 & B3. The base case named Case 0 is the one with-

out a baffle. Ten cases from Case 0 to Case 9 have been calculated for each selected mass flow. In total 50 simulations have been performed.

Mesh sensitivity studies have been performed to determine the influence of mesh coarseness and the number of iterations on value of average residence time. Mesh coarseness is prescribed by the factor base size, from

Table 1. Different mesh sizes and their characteristics

	Cells	Interior faces	Vertices
Base size 0.1 m	1621	9838	9164
Base size 0.08 m	3357	21151	19438
Base size 0.06 m	6574	42643	38742

which all other mesh related values are derived. Three base sizes were taken into consideration, *i. e.*: 0.1 m, 0.08 m and 0.06 m. The characteristics of the meshes, number of cells, interior faces and vertices are given in tab. 1.

The analysis is given for three characteristic cases: 0 (fig. 5), 3 (fig. 6), and 9 (fig. 7), where by 6, 8, and 10 are denoted base sizes 0.06, 0.08, and 0.10. The chosen mass flow for the mesh sensitivity analysis was 0.16 kg/s.

The analysis is given for three characteristic cases: 0 (fig. 5), 3 (fig. 6), and 9 (fig. 7), where by 6, 8, and 10 are denoted base sizes 0.06, 0.08, and 0.10. The chosen mass flow for the mesh sensitivity analysis was 0.16 kg/s.

The results show that the solutions converge, and that the coarsest mesh at 2000 iterations gives results that are satisfactory close to the results of all three meshes at 4000 iterations (differences range from 0.1 s for the Case 0, to 0.25 s for the Case 9).

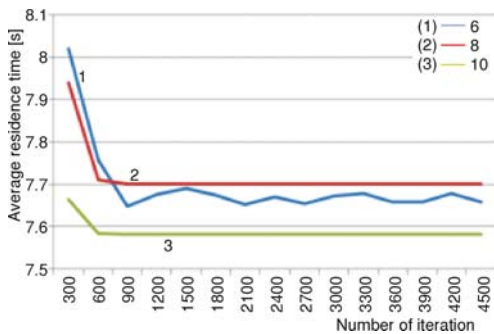


Figure 5. Mesh sensitivity for the Case 0

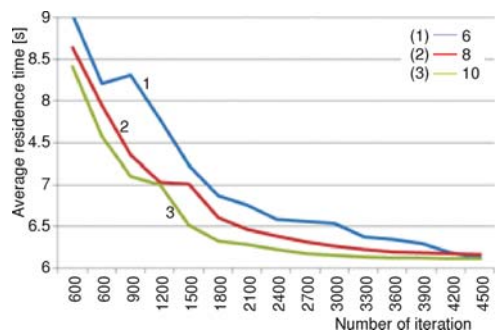


Figure 6. Mesh sensitivity for the Case 3

Results and discussion

In the tab. 2. and the fig. 8. results from the average residence time calculation are presented.

In tab. 3 and fig. 9 are represented the same results as in tab. 2 and fig. 8, just in relative values. The base value is the residence time for the Case 0. These results show that baffles can cause an increase as well as a decrease of the residence time when installed. Values range from -17 percentage points to +13 for the CFD tested designs change relative to the case without baffles.

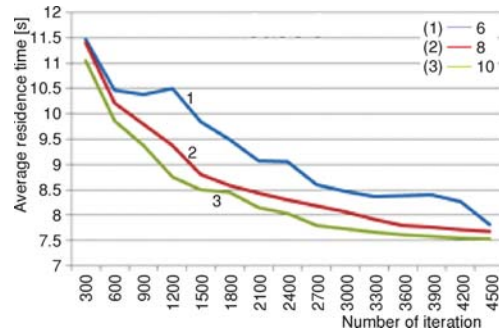


Figure 7. Mesh sensitivity for the Case 9

Table 2. Average residence time for different geometries and mass flows

Average residence time [s]	Mass flow [kgs ⁻¹]				
	0.16	0.24	0.32	0.4	0.48
Case 0	7.62	5.08	3.81	3.05	2.55
Case 1	6.97	4.61	3.49	2.79	2.32
Case 2	6.54	4.37	3.28	2.62	2.18
Case 3	6.51	4.26	3.19	2.55	2.12
Case 4	7.35	4.88	3.67	2.95	2.45
Case 5	7.23	4.82	3.62	2.89	2.41
Case 6	7.32	4.83	3.61	2.88	2.40
Case 7	7.94	5.28	3.95	3.15	2.61
Case 8	8.14	5.29	3.91	3.14	2.61
Case 9	8.65	5.70	4.25	3.35	2.73
<i>t_{calc. Case 0}*</i>	7.40	4.93	3.70	2.96	2.47
$\frac{t_{calc. Case 0} - t_{CFD Case 0}}{t_{CFD Case 0}}$ **	-0.03	-0.03	-0.029	-0.031	-0.035

* $t_{calc. Case 0} = V / (\dot{m} / \rho_{Air})$, where, V , \dot{m} and ρ_{Air} are volume of the combustion chamber, air mass flow and air density (1.18415 kg/m³)
 ** Differences appear as a result of influence on the average value of the tracks which end in a re-circulation flows

Table 4 shows the influence of the baffle length on the residence time at different positions. For the case of baffles at the lowest position, a sharp drop in residence time is present with an increase of length, while at the medium height values vary slightly, and at the highest position a sharp rise is present.

Table 5 shows the influence of the baffle position on residence time for different baffle lengths. At all lengths there is a trend of increase of the residence time when the baffle is installed higher. The longer the baffle the greater this increase is.

Figures 10, 11, and 12 present particle tracks for cases 0, 3, and 9. Here tracks are colored depending on the residence time value. These cases are chosen as they represent the base

Table 3. Average residence time for different geometries and mass flows presented in relative units (base case Case 0 – baffles case)

t_{rel1}^*	Mass flow [kgs ⁻¹]				
	0.16	0.24	0.32	0.40	0.48
Case 1	-8.5	-9.3	-8.4	-8.5	-9.0
Case 2	-14.2	-14.0	-13.9	-14.1	-14.5
Case 3	-14.6	-16.1	-16.3	-16.4	-16.9
Case 4	-3.5	-3.9	-3.7	-3.3	-3.9
Case 5	-5.1	-5.1	-5.0	-5.2	-5.5
Case 6	-3.9	-4.9	-5.2	-5.6	-5.9
Case 7	4.2	3.9	3.7	3.3	2.4
Case 8	6.8	4.1	2.6	3.0	2.4
Case 9	13.5	12.2	11.5	9.8	7.1

* Relative residence time $t_{rel1} = (t_{CFD \text{ Case } i} - t_{CFD \text{ Case } 0}) / t_{CFD \text{ Case } 0}$

Table 4. Influence of baffle length on relative average residence time

Baffle	Relative average residence time, t_{rel2}^* [%]	Mass flow [kgs ⁻¹]				
		0.16	0.24	0.32	0.40	0.48
Position 1	Case 1	0	0	0	0	0
	Case 2	-6.2	-5.2	-6.1	-6.1	-6.0
	Case 3	-6.6	-7.4	-8.4	-8.6	-8.7
Position 2	Case 4	0	0	0	0	0
	Case 5	-1.6	-1.2	-1.5	-1.9	-1.7
	Case 6	-0.3	-1.1	-1.7	-2.2	-2.1
Position 3	Case 7	0	0	0	0	0
	Case 8	2.5	0.4	-1.0	-0.3	0
	Case 9	9.0	8.0	7.5	6.6	4.7

* $t_{rel2} = (t_{calc. \text{ case } i} - t_{calc. \text{ base case}}) / t_{calc. \text{ base case}}$; base case is always the first case at the given vertical position, i. e. Case 1, Case 4, and Case 7

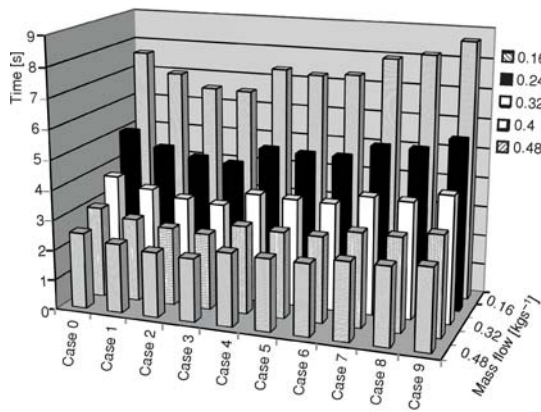


Figure 8. Average residence time for different geometries and mass flows

case, worst case, and the best case. The presented data are for the mass flow of 0.16 kg/s, and for the maximal residence time of 10 s. These figures explain the previous results, in which best case was Case 9 and the worst case Case 3. On fig. 11 a significant re-circulation zone above the baffle is present which influences the effective zone of the furnace.

In figs. 13, 14, and 15 velocity fields for cases 0, 3, and 9 are presented, for the mass flow 0.16 kg/s. Velocity fields are represented for the central cross-section that halves the fur-

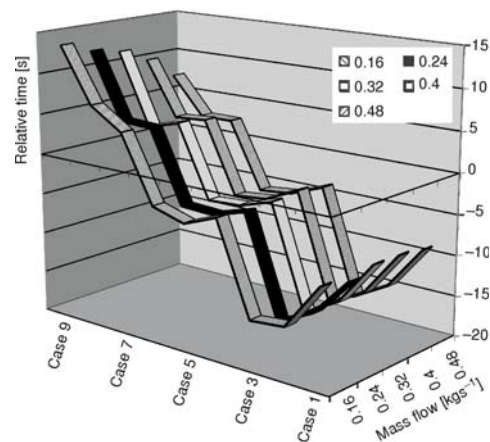


Figure 9. Average residence time for different geometries and mass flows presented in relative units (base case Case 0 – unbaffled case)

Table 5. Influence of baffle position on relative average residence time**

Baffle	Relative average residence time [%] t_{rel2}^*	Mass flow [kgs ⁻¹]				
		0.16	0.24	0.32	0.40	0.48
Length 1	Case 1	0	0	0	0	0
	Case 2	5.4	6.0	5.3	5.7	5.5
	Case 7	13.8	14.5	13.3	12.8	12.2
Length 2	Case 2	0	0	0	0	0
	Case 5	10.6	10.5	10.4	10.4	10.3
	Case 8	24.5	21.3	19.4	19.8	19.3
Length 3	Case 3	0	0	0	0	0
	Case 6	12.4	13.2	13.0	13.0	13.1
	Case 9	32.8	33.6	33.1	31.5	28.6

** Base case is always the first case of the given length, *i. e.* Case 1, Case 2 and Case 3

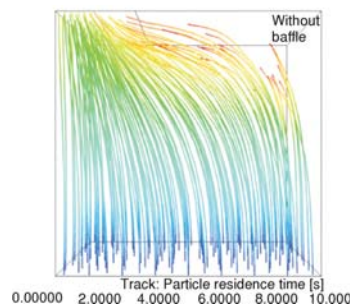


Figure 10. Particle tracks for Case 0

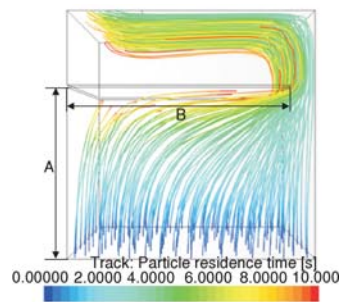


Figure 11. Particle tracks for Case 3

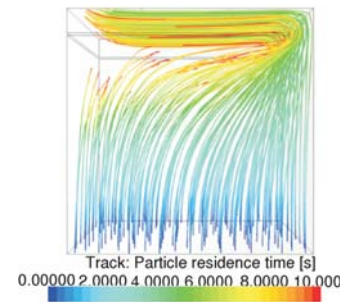


Figure 12. Particle tracks for case 9

nance volume. Re-circulation zone is evident on fig. 14 above the baffle. Therefore, analysis of fig. 11 is confirmed.

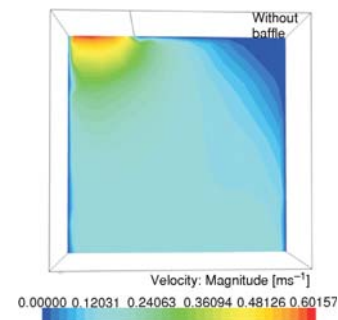


Figure 13. Velocity field for Case 0

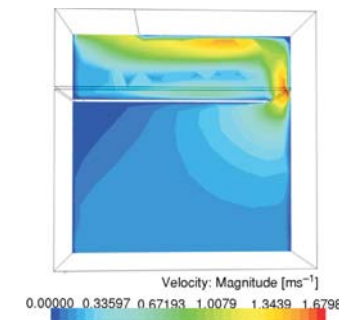


Figure 14. Velocity field for Case 3

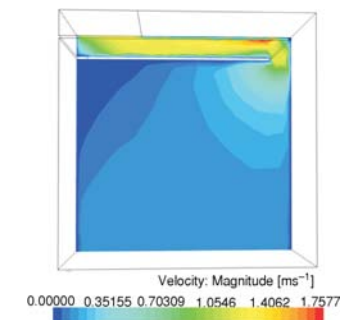


Figure 15. Velocity field for Case 9

The practice in Serbia shows that small boiler producers prefer not to use this measure. One can assume that tests could have been done with unsatisfactory results. The first reason for that is the increase in pressure drop. Baffles are in a way like a throttling device for hot gases. Therefore, in order to have the same air flow, the higher chimney has to be built or a fan must be installed. Without these measures, the situation deteriorates in respect of heat output. The second reason is concerning hot gas temperatures. As additional time is provided for their flow in a furnace, they can be cooled below the ignition temperature. In that case, even the perfect mixing and high excess air will not lead to combustion. This case is more realistic, since high excess air ratio leads to lower the adiabatic flame temperature. Water-cooled furnace walls additionally cool furnace. The recommendation for this case would be to introduction of lining is recommended, in order to prevent gas cooling below the ignition temperature. The lining should not cover the whole furnace. The preceding analysis points out the complexity of the problem. It states the factors that could cause negative effects of baffle installment. Apart from that, however, results presented in this paper show that also correctly sized and positioned baffles are important design variables. Baffles can cause residence time increase and combustion improvement only if properly installed.

Conclusions

For chemical reactors the residence time is an important factor, as it is for a boiler, whose combustion chamber is a reactor itself. The usual design of combustion chambers is of a prismatic form, with or without baffles. There are dead zones in which re-circulation eddies form, and decrease the effective volume of chamber, simultaneously decreasing the residence time. There is no formula to predict the extent of dead zones. The traditional way of measuring the residence time is by the tracer analysis. The applicability in the domain of combustion is somewhat difficult as, in contrast to chemical reactors, reactions do not take place in minutes or hours range, but in seconds. The usage of CFD and the virtual tracer massless particle are becoming a standard tool. Massless particle is an "ideal" tracer as it does not influence the flow at all, nor does it mix with it, or react with it. In this paper, the use of baffles in a combustion chamber, as one well-known technology for the combustion improvement, was put on test since there are no recommendations of its proper installation in regular textbooks and peer-reviewed papers. The results from the simplified model show that the most important variable is the vertical positioning of the baffle, whereas the length can increase and decrease the residence time. Having in mind these results, it is an open question whether boilers in Serbia in low-cost segment, which do not use this measure, should continue this practice.

Acknowledgments

This work has been done in the frame of the project "Development of methods, sensors and systems for monitoring of quality of water, air and land", for the Ministry of Education, Science and Technological Development of the Republic of Serbia (Project No III 43008).

Nomenclature

G	– generation of turbulent kinetic energy	S_ε	– source term for ε
k	– turbulent kinetic energy, [m^2s^{-2}]	\mathbf{T}_t	– Reynolds stress tensor, [$\text{kgm}^{-1}\text{s}^{-2}$]
p	– pressure, [$\text{kgm}^{-1}\text{s}^{-2}$]	u_i	– mean velocity components, [ms^{-1}]
S_k	– source term for k	u'_i	– fluctuating velocity components, [ms^{-1}]

Greek symbols

ε	– dissipation rate of turbulent kinetic energy [m^2s^{-3}]	ρ	– density, [kgm^{-3}]
μ_t	– turbulent viscosity, [$\text{kgm}^{-1}\text{s}^{-1}$]	σ_ε	– turbulent Prandtl number for ε [–]
		σ_k	– turbulent Prandtl number for k [–]

References

- [1] Ebeling, J., Jenkins, B., Thermochemical Properties of Biomass Fuels, Agricultural and Natural Resources Communication Services webservice, <http://ucce.ucdavis.edu/files/repositoryfiles/ca3905p14-62863.pdf>
- [2] Domalski, E., et al., Thermodynamic Data for Biomass Conversion and Waste Incineration, Technical Report No.: SERI/SP-271-2839, National Bureau of Standards, Boulder, Cal., USA, 1986
- [3] Martinov, M., et al., Efficiency and Emission of Crop Residues Combustion Facilities in Serbia – Status and Needed Measures for Improvement, *Thermal Science*, 10 (2006), 4, Suppl., pp. 189-194
- [4] Pešenjanski, I., Stepanov, B., Test Results for a 250 kW Bio-Mass Energy Boiler and Suggested Technical and Organizational Measures to Increase Energy Efficiency of Current Boiler Installations, *Savremena poljoprivredna tehnika*, 30 (2005), 4, pp. 197-203
- [5] Wick, O, Wik, M., *Wood Stoves : How to Make and Use Them*, Northwest Pub. Co. Anchorage, Alas., USA, 1977
- [6] Trinks, W., et al., *Industrial Furnaces*, 6th ed., John Wiley and Sons, Inc., Hoboken, N. J., USA, 2004
- [7] Nasserzadeh, V., et al., Effects of High Speed Jets and Internal Baffles on the Gas Residence Times in Large Municipal Incinerators, *Environmental Progress*, 13 (1994), 2, pp. 124-133
- [8] Shelton, J., *Jay Shelton's Solid Fuels Encyclopedia*, Garden Way Publishing, Charlotte, Vt., USA, 1983
- [9] Kreuh, L., *Steam Generators* (in Croatian), Školskknjiga, Zagreb, Croatia, 1978
- [10] Hartmann, H., et al., *Handbook, Bioenergy – Small Scale Plants* (in German), Fachagentur Nachwachsende Rohstoffe e. V. (FNR), http://www.tfz.bayern.de/sonstiges/17745/handbuch_komplett.pdf
- [11] Dimaczek, G., et al., Small Scale Combustion Plant for Cereal and Straw. Final Report for Specialized Agency for Renewable Resources Registered Association Gulzow (in German), ATZ Entwicklungszentrum, <http://www.fnr-server.de/ftp/pdf/berichte/22019303.pdf>
- [12] Eltrop, L., et al., Recommendation Bioenergy – Planning, Operating and Economy of Bioenergy Plants (in German), Fachagentur Nachwachsende Rohstoffe, http://fnr-server.de/cms35/fileadmin/biz/pdf/leitfaden/leitfaden_bioenergie.pdf
- [13] Scott, A. J., Real-Life Emissions from Residential Wood Burning Appliances in New Zealand, <http://ecan.govt.nz/publications/Reports/air-report-emissions-residential-wood-burning-appliances-nz-000805.pdf>
- [14] Todd, J. J., Research Relating to Regulatory Measures for Improving the Operation of Solid Fuel Heaters, Eco-Energy Options, Prepared for the New South Wales Department of Environment and Conservation, http://www.environment.nsw.gov.au/resources/woodsmoke/execsummary_todreport.pdf
- [15] ***, *Handbook of Biomass Combustion and Co-Firing*, (Eds. S. Van Loo, J. Koppejan) Twente University Press, Twente, The Netherlands, 2002
- [16] Beer, J. M., Lee, K. B., The Effect of the Residence Time Distribution on the Performance and Efficiency of Combustors, 10th Symposium (International) on Combustion, *Proceedings*, The Combustion Institute, Cambridge, UK, 1965, 1, pp. 1187-1202
- [17] Swithenbank, J., et al., Combustion Design Fundamentals, 14th Symposium (International) on Combustion, *Proceedings*, The Combustion Institute, Altona, Penn., USA, 1973, 1, pp. 627-638
- [18] Han, J-H., et al., A Hot-Flow Model Analysis of the MSW Incinerator, *International Journal of Energy Research*, 21 (1997), 10, pp. 899-910
- [19] Fehr, M., Vaclavinek, J., A Cold Model Analysis of Solid Waste Incineration, *International Journal of Energy Research*, 16 (1992), 4, pp. 277-283
- [20] Choi, S., et al., Cold Flow Simulation of Municipal Waste Incinerators, 25th Symposium (International) on Combustion, Irvine, Cal., USA, *Proceedings*, The Combustion Institute, Pittsburgh, Penn., USA, 1994, pp. 317-323
- [21] Ravichandran, M., Gouldin, F.C., Numerical Simulation of Incinerator Overfire Mixing, *Combustion Science and Technology*, 85 (1992), 1-6, pp. 165-185

- [22] Nasserzadeh, V., Swithenbank, J., Design Optimization of a Large Municipal Solid Waste Incinerator, *Waste Management*, 11 (1991), 4, pp. 249-261
- [23] Nasserzadeh, V., *et al.*, Effects of High Speed Jets and Internal Baffles on the Gas Residence Times in Large Municipal Incinerators, *Environmental Progress*, 13 (1994), 2, pp. 124-133
- [24] ***, Personal Communication with Ph. D. mentor professor Pešenjanski
- [25] Seeker, W. R., *et al.*, Municipal Waste Combustion Study: Combustion Control of MSW Combustors to Minimize Emission of Trace Organics, Technical report: EPA/530-SW-87-021x, EPA, NY, US, 1987
- [26] ***, Star CCM+ manual, CD-Adapco. Melville, NY, USA
- [27] Brkić, Lj., Živanović, T., Thermal Calculation of Steam Boilers (in Serbian), Mašinski Fakultet, Belgrade, Serbia, 1984